

early flowering phenotype¹⁸ (B. Savidge, S. Rounsley and M.F.Y., unpublished results).

Because ectopic *API* activity reduces the vegetative phase of the life cycle of a plant, it is clearly influencing the behaviour of the vegetative meristem. However, ectopic expression of *API* alone is unable to convert the vegetative apical meristem into a flower immediately after germination. These data suggest that additional floral-promoting factors present in the inflorescence meristem are required for this conversion or, alternatively, that floral-inhibiting factors present in the vegetative meristem prevent this conversion. Whether or not the early flowering phenotype is a direct consequence of *API* acting at the vegetative shoot apex, or is an indirect result of altered plant growth and metabolism caused by the altered activity of downstream genes regulated by *API*, remains to be determined. However, the ability to control flowering time by ectopic *API* expression should prove a useful tool, not only for investigating the factors that regulate floral induction, but also for reducing the time to flowering of agriculturally important crop plants. □

Received 29 August; accepted 18 September 1995.

1. Weigel, D. A. *Rev. Genet.* **29**, 19–39 (1995).
2. Yanofsky, M. F. A. *Rev. Pl. Physiol. molec. Biol.* **46**, 167–188 (1995).
3. Weigel, D., Alvarez, J., Smyth, D. R., Yanofsky, M. F. & Meyerowitz, E. M. *Cell* **69**, 843–859 (1992).
4. Mandel, M. A., Gustafson-Brown, C., Savidge, B. & Yanofsky, M. F. *Nature* **360**, 273–277 (1992).
5. Jofuku, K. D., den Boer, B. G. W., Van Montagu, M. & Okamoto, J. K. *Pl. Cell* **6**, 1211–1225 (1994).
6. Kempin, S. A., Savidge, B. & Yanofsky, M. F. *Science* **267**, 522–525 (1995).
7. Levin, J. & Meyerowitz, E. M. *Pl. Cell* **7**, 529–548 (1995).
8. Odell, J. T., Nagy, F. & Chua, N.-H. *Nature* **313**, 810–812 (1985).
9. Shannon, S. & Meeks-Wagner, D. R. *Pl. Cell* **3**, 877–892 (1991).
10. Alvarez, J., Gulik, C. L., Yu, X.-H. & Smyth, D. R. *Pl. J.* **2**, 103–116 (1992).
11. Shannon, S. & Meeks-Wagner, D. R. *Pl. Cell* **5**, 639–655 (1993).
12. Schuit, E. A. & Haughn, G. W. *Pl. Cell* **3**, 771–781 (1991).
13. Huala, E. & Sussex, I. M. *Pl. Cell* **4**, 901–913 (1992).
14. Weigel, D. & Nilsson, O. *Nature* (in the press).
15. Gustafson-Brown, C., Savidge, B. & Yanofsky, M. F. *Cell* **76**, 131–143 (1994).
16. Irish, V. F. & Sussex, I. M. *Pl. Cell* **2**, 741–751 (1990).
17. Bowman, J. L., Alvarez, J., Weigel, D., Meyerowitz, E. M. & Smyth, D. R. *Development* **119**, 721–743 (1993).
18. Chung, Y. Y., Kim, S.-R., Finkel, D., Yanofsky, M. F. & An, G. *Pl. molec. Biol.* **26**, 657–776.
19. Jack, T., Fox, G. L. & Meyerowitz, E. M. *Cell* **76**, 703–716 (1994).
20. Bechtold, N., Ellis, J. & Pelletier, G. C. R., *C. r. hebdo. Séanc. Acad. Sci., Paris* **316**, 1194–1199 (1993).

ACKNOWLEDGEMENTS. We thank D. Weigel for helpful discussions and sharing unpublished data, and S. Liljegren and C. Fankhauser for comments on the manuscript. This work was supported by the National Science Foundation.

Requirement for *Drosophila* cytoplasmic tropomyosin in *oskar* mRNA localization

Miklós Erdélyi, Anne-Marie Michon, Antoine Guichet, Jolanta Bogucka Glotzer & Anne Ephrussi*

European Molecular Biology Laboratory, Meyerhofstrasse 1, 69117 Heidelberg, Germany

THE localization of *oskar* (*osk*) RNA to the posterior pole of the developing fruit fly (*Drosophila*) oocyte induces the assembly of pole plasm, causing development of the abdomen and germ line^{1,2}. Failure to localize *oskar* RNA results in embryos that lack abdomen and germ cells. Conversely, mis-targeting of *oskar* RNA to the anterior of the oocyte causes formation of ectopic abdomen and germ cells at the anterior pole³. Maternal mutants that have reduced pole plasm activity produce sterile adults with normal abdominal development, suggesting that germ cells are more sensitive than abdomen to defects in pole plasm assembly⁴. Thus muta-

tions in genes that reduce *oskar* RNA localization or activity can be recovered as viable sterile adults. In a screen for mutants defective in germ cell formation, we isolated nine alleles of the tropomyosin II gene⁵. Here we show that mutations in *tropomyosin II* (*TmII*) virtually abolish *oskar* RNA localization to the posterior pole, suggesting an involvement of the actin network in *oskar* RNA localization.

Embryos derived from *TmII*^{gs1} females fail to form pole cells, the precursors of the germ cells (Fig. 1a, b), and develop into sterile adults. In the three molecularly characterized lines (*TmII*^{gs1}, *TmII*^{gs2} and *TmII*^{gs3}), the transposable element has inserted in the *TmII* gene, immediately downstream of the first exon of the cytoplasmic form of tropomyosin (cTm)^{5,6}. cTm is expressed exclusively in the ovary, where it is the major *TmII* isoform detected⁵. Northern analysis reveals that the level of cTm transcripts is reduced in *TmII*^{gs1} mutant ovaries (Fig. 1e).

To determine whether *TmII*^{gs1} mutants are sterile through a defect in pole plasm assembly or in pole cell formation *per se*, we assayed the ability of anteriorly localized *osk* RNA (ref. 3) to induce pole cells at the anterior pole in the *TmII*^{gs1} mutant

TABLE 1 Germline clone analysis of lethal excisions of *TmII*^{gs1}

Allele	Clones per female (n)	Eggs per female	Embryos with posterior phenotype	Viable adult progeny
+	0.35 (450)	9.6	—	—
el3	0.14 (653)	2.7*	+	+
el4	0.16 (434)	4.3	+	+
er4	0.13 (508)	3.2*	+	+

Mosaic egg chambers composed of homozygous mutant germ cells and heterozygous follicle cells reproduce the germ-cell-less phenotype of the original *TmII*^{gs} mutants. Conversely, mosaic egg chambers produced by transplantation of wild-type pole cells into homozygous *TmII*^{gs} embryos result in wild-type egg chambers and wild-type embryos (J. Szabad, personal communication). Taken together, these results show that the *TmII* germ-cell-less phenotype is germline-dependent. The average number of clones per female was calculated by the Poisson distribution. We also observed a small but significant reduction in the number of eggs in the mutants, indicating a partial cell-lethal effect of the *TmII* lethal alleles in the germ line. The *TmII*^{gs} mutations were isolated as homozygous viable PLacZ (w⁺) insertions²². The transposon was mobilized from the X chromosome with a *trans* transposase source, the Δ2-3 element. The new autosomal insertion-bearing male individuals were selected for their w⁺ eye colour. Stable insertional lines were established with the T(2,3)CyO l(2)513 TM2 Ultrabithorax (Ubx) translocated balancer chromosome. From each line, females homozygous for new PLacZ insertions were collected based on the absence of dominant markers of the translocated balancer chromosome. Germ-cell-less mutant lines were selected on the basis of sterility of the progeny of homozygous females. Analysis was carried out with *TmII*^{gs1}, *TmII*^{gs2} and *TmII*^{gs3}, from which the 5' and 3' genomic flanking regions of the inserted PLacZ elements were cloned by plasmid rescue²². A minimum of 150 base pairs (bp) of DNA flanking the PLacZ elements was sequenced using a primer derived from the P-element inverted repeat and bears 100% identity to sequences within the fourth exon and the 5' region of the fourth intron of the *TmII* gene. *TmII*^{gs1}, *TmII*^{gs2} and *TmII*^{gs3} are insertions at positions 3,753, 3,753 and 3,737 of the *TmII* genomic sequence²³, respectively. In *TmII*^{gs1}, the PLacZ element was remobilized, generating wild-type, grandchildless, as well as homozygous lethal excision alleles of the *TmII* gene. The lethal excisions *TmII*^{el3}, *TmII*^{el4} and *TmII*^{er4} were used to generate X-ray-induced homozygous germ-line clones. The *TmII*^{gs} insertions were mapped to the 88F chromosomal region. Df(3R)ea^{5022RX1}, an 88F overlapping deficiency, does not complement the *TmII*^{gs} mutations and the hemizygotes show a phenotype identical to that of homozygotes. Germline clones of lethal *TmII* alleles in *trans* to the dominant female sterile insertion *P[ovo^{D1}]* on chromosome 3R were induced by X-rays²⁴. *P[ovo^{D1}]/TmII* lethal heterozygotes were irradiated (1,000 rad, 150 rad min⁻¹, 150 kV) at 72±3 h after egg laying²⁵. The irradiated females were collected as virgins and mated with Oregon R (wild-type) males. Egg production of groups of 10 irradiated females were recorded over 12 days.

* $P < 0.05$; χ^2 -test.

* To whom correspondence should be addressed.

background. Embryos derived from *osk-bicoid*; *TmII^{gs1}*/*TmII^{gs1}* females form pole cells at the anterior (Fig. 1c, d). This indicates that the *TmII^{gs1}* mutation does not affect germ cell formation *per se*. Rather, localization or maintenance of pole plasm molecules at the posterior pole is defective in *TmII^{gs1}* mutants. Indeed, when embryos from mutant females are greatly overstained with an antibody against the *osk* protein, only a trace amount of *osk* protein is observed, exclusively at the posterior pole (data not shown). Nonetheless, a gradient of *nanos* protein is formed (data not shown) and abdomen development is normal in 98% of embryos from *TmII^{gs1}* homozygous females, leading to viable but sterile adults.

To investigate whether stronger mutant alleles of *TmII* might have a more dramatic effect on oocyte development, we carried out germline clonal analysis with lethal alleles generated by excision of the P element from the original allele, *TmII^{gs1}*. As shown in Table 1, germ cells homozygous mutant for the lethal *TmII* alleles give rise to viable egg chambers that on fertilization develop into sterile adults, as well as to embryos that show abdominal defects. Hence, germline clones of lethal *TmII* mutations have a phenotype similar to that of *TmII^{gs1}*. This result suggests that *TmII* function is specific for pole plasm formation during oogenesis.

Localized *osk* RNA is required to induce assembly of a functional posterior pole plasm^{1,2}. During the early stages of oogenesis, *osk* RNA is enriched in the oocyte. At stage 8, *osk* RNA shows a transient anterior accumulation and the onset of posterior localization. By stage 9, *osk* RNA is present exclusively at the posterior pole. In *TmII^{gs1}* mutants, the initial enrichment of *osk* RNA in the oocyte is normal, but translocation of the RNA to the posterior pole fails (Fig. 2a, b). Instead, at stage 8, *osk* RNA accumulates at the anterior margin of the oocyte, where it remains until stage 10. The *staufer* gene (*stau*)⁷ is required for *osk* RNA localization, and in wild-type oocytes, RNA-binding protein STAU colocalizes with *osk* RNA. In the *TmII^{gs1}* mutants, STAU distribution precisely parallels that of *osk* RNA (Fig. 2c, d). The *TmII^{gs1}* defect seems to be specific to the posterior localization pathway, as the anterior localization of *bcd* and the anterior-dorsal localization of *gurken* (*grk*) are not perturbed (Fig. 2e-h).

The general importance of the cytoskeleton in RNA localization has been shown in a variety of organisms. Localized RNAs such as *Vg1* in *Xenopus* and *bcd orb*, *fs(1)K10*, *BicaudalD* and *osk* RNAs in *Drosophila* are enriched in detergent-resistant cytoskeletal fractions^{8,9}. *In vivo*, cytochalasin, an inhibitor of actin polymerization, prevents localization of *actin* mRNA to the per-

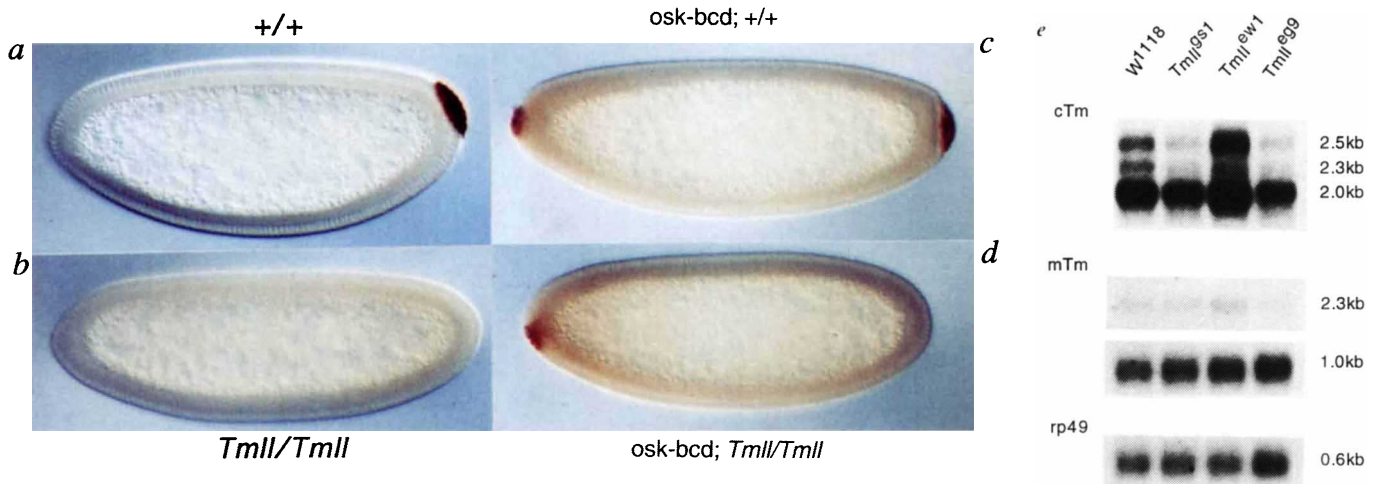


FIG. 1. Cytoplasmic tropomyosin is required for pole cell formation. a, b, Pole cells form at the posterior pole of wild-type embryos (a), but fail to form in embryos from *TmII^{gs1}/TmII^{gs1}* mutant females (b). c, d, Pole cells form at both poles in embryos from *osk-bcd3 UTR* females (c), but form exclusively at the anterior of embryos from *osk-bcd3 UTR; TmII^{gs1}/TmII^{gs1}* females. Embryos from *osk-bcd3 UTR* and *osk-bcd3 UTR; TmII^{gs1}/TmII^{gs1}* females form two abdomens of opposite polarity (data not shown). a–d, Pole cells are stained with an anti-NANOS antibody. a, b, Embryos at early cellular blastoderm stage; c–d, embryos at late syncytial blastoderm stage. All embryos orientated anterior left, dorsal up. The genotypes refer to that of the mothers from which the embryos are derived. e, cTm transcripts are reduced in *TmII* mutant ovaries. Northern blot bearing poly(A)⁺ RNA isolated from ovaries of *w¹¹¹⁸* (wild-type), *TmII^{gs1}* as well as *TmII^{ew1}* and *TmII^{eg9}*, two lines generated by excision of the P element from *TmII^{gs1}*. Mutants are described in Table 1 legend. *TmII^{eg9}* has the original *gs* phenotype of *TmII^{gs1}*, and *TmII^{ew1}* is a revertant to the wild type. When probed with a cTm-specific probe (upper panel) *TmII^{gs1}* and *TmII^{eg9}* reveal reduced levels of cTm transcripts, whereas the revertant *TmII^{ew1}* shows an increase in cTm transcripts to levels greater than *w¹¹¹⁸*. A muscle-specific probe (mTm) (middle panel) shows that the *TmII* mutations do not significantly affect the muscle transcripts detected. A probe specific for ribosomal protein 49 (rp49) (lower panel) serves as loading control. *TmII* is a complex gene, producing a large array of messenger RNAs by alternative splicing and differential polyadenylation. In addition, it is likely that several additional spliced transcripts exist that have not been identified or characterized²⁶. We have not yet determined the precise molecular

nature of the three (2.0, 2.3, and 2.5 kilobases (kb)) cTm transcripts, but presume they correspond to the 2.0-, 2.2- and 2.4-kb²⁶ and the 2.0-, 2.3- and 2.8-kb⁵ transcripts previously described, whose molecular nature is not fully understood. The 1.0-kb mTm transcript we detect using a probe specific for exons 1–3 may correspond to the 1.4-kb mRNA previously described⁵, or may represent an additional transcript. No 2.3-kb mTm mRNA has previously been reported, but this transcript is specific, as its amount increases in the revertant, and it is clearly distinct from cTm, because its profile differs from that of the cTm transcripts in the mutants.

METHODS. Whole-mount antibody staining of embryos was carried out as described elsewhere³. Nomarski optics. Poly(A)⁺ RNA (from 150 µg total RNA) was isolated from *w¹¹¹⁸* (wild-type), *TmII^{gs1}*, *TmII^{ew1}* and *TmII^{eg9}* mutant ovaries dissected in cold EB Ringer's, resolved on a 1.5% formaldehyde-agarose gel and blotted onto nitrocellulose. Hybridization was carried out at 55 °C in 50% formamide, 0.25 M NaPO₄ pH 7.2, 0.25 M NaCl, 1 mM EDTA, 7% SDS. cTm riboprobe: A *HindIII*–*XbaI* 0.55-kb fragment corresponding to exon 4 of *TmII* (bp 3,042–3,594) (ref. 23) was generated by polymerase chain reaction (PCR; information on primer sequences available on request) and subcloned into pSP72. Genomic DNA flanking the P element was isolated by plasmid rescue and served as template for the PCR. mTm riboprobe: A *HindIII*–*BglII* 0.31-kb fragment, covering exons 1–3 (bp 471–1,410; ref. 23), was generated by PCR from the mTm cDNA and subcloned into pSP72. rp49 riboprobe: A 0.42-kb PCR-generated fragment (407–571 bp²⁷) was subcloned into pBSK⁺. *In vitro* transcription of riboprobes was from the T7 promoter.

iphery in chicken fibroblasts¹⁰ and causes the release of localized *Vg1* mRNA from the vegetal pole of *Xenopus* oocytes¹¹. The microtubule drugs nocodazole, colchicine and taxol interfere with the translocation of *Vg1* RNA in *Xenopus*¹¹, and with localization of *bcd*, *orb*, *fs(1)K10*, *BicaudalD* and *osk* mRNAs in *Drosophila*^{12–14} oocytes, respectively. We therefore examined the organization of the cytoskeleton in *TmII^{gs1}* mutant ovaries. In *TmII^{gs1}* egg chambers, the filamentous actin network, revealed with rhodamine-conjugated phalloidin, seems to be normal (Fig. 3a, b). The distribution of microtubules also appears normal in *TmII^{gs1}* oocytes, as visualized with an anti- α -tubulin antiserum (data not shown). In addition, two microtubule motor proteins, dynein heavy chain (Dhc64C)¹⁵ (Fig. 3c, d) and a kinesin- β -galactosidase fusion protein¹³ (data not shown) are properly localized to the posterior pole of *TmII^{gs1}* oocytes. Ooplasmic streaming, a process that requires intact microtubules¹⁶, occurs in the mutant as in the wild type. As the actin microfilament and microtubule networks, the distribution of microtubule motor proteins and the process of ooplasmic streaming seem to be normal, we conclude that the overall integrity of the cytoskeleton is intact in *TmII^{gs1}*.

Our data show a role for cTm in *osk* RNA localization. Tropomyosin proteins are involved in actin-based motility in muscle cells, and cytoplasmic tropomyosin has been shown to associate with actin in non-muscle cells (reviewed in refs. 17, 18). In this context, our findings raise the possibility of an involvement of the actin cytoskeleton in RNA localization in the oocyte, a process in which microtubules have previously been implicated. We can envisage two ways in which cTm might function in this context. cTm protein might be an obligate component of a complex coupling *osk* RNA to putative microtubule-dependent motors that mediate its transport to the posterior pole. This model is supported by the observation that the *TmII^{gs1}* mutation uncouples the localization of *osk* RNA from that of the microtubule motor proteins dynein and kinesin- β -galactosidase. Alternatively, both actin and microtubule cytoskeletons might be required for *osk* RNA localization to the posterior pole. In support of this view, there is increasing evidence for functional interaction between the actin and microtubule cytoskeletal networks (for a review see ref. 19). For example, membranous organelles have been shown to move on both actin filaments and microtubules in squid axoplasm²⁰. In view of the possible involvement of

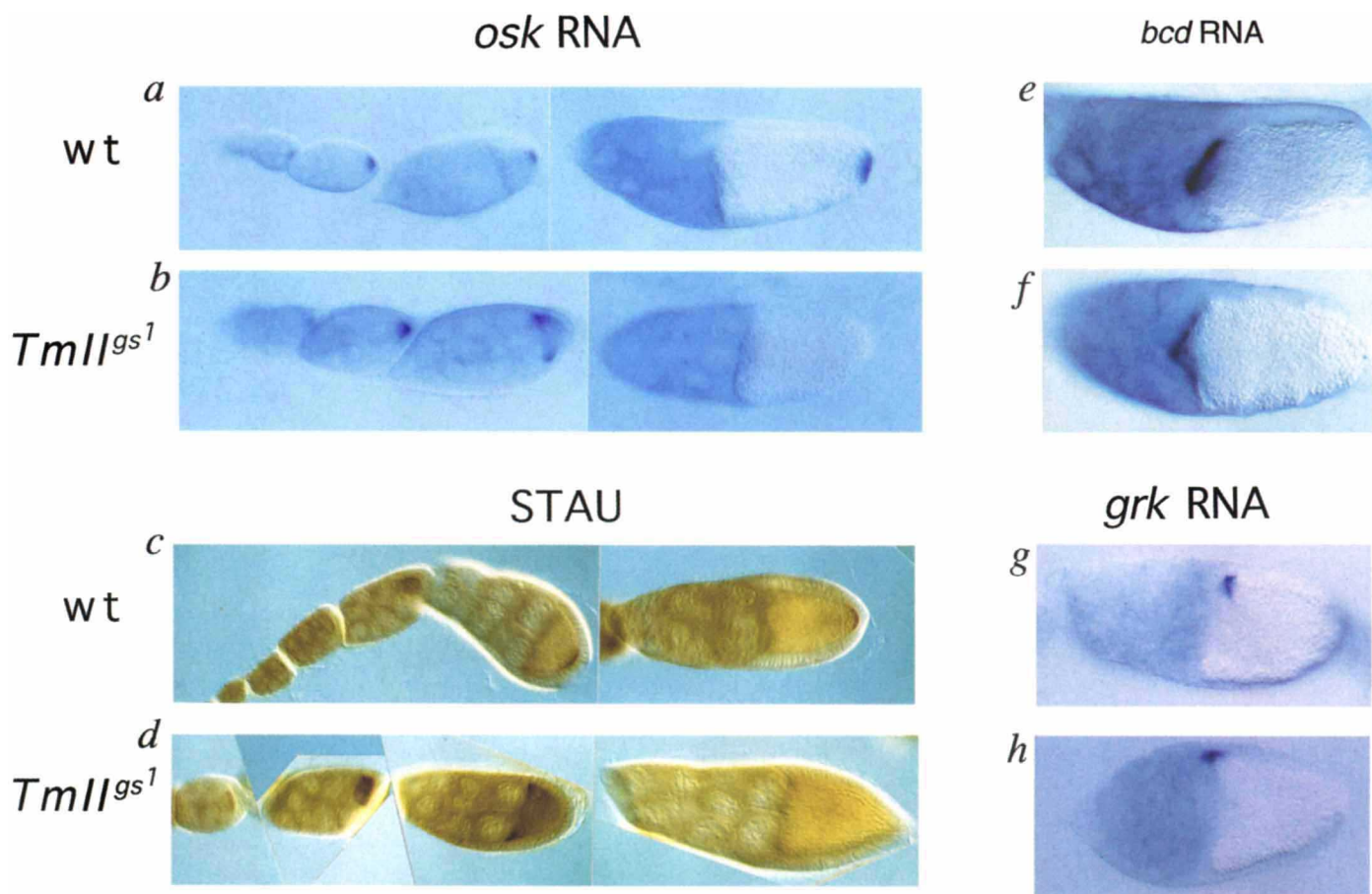
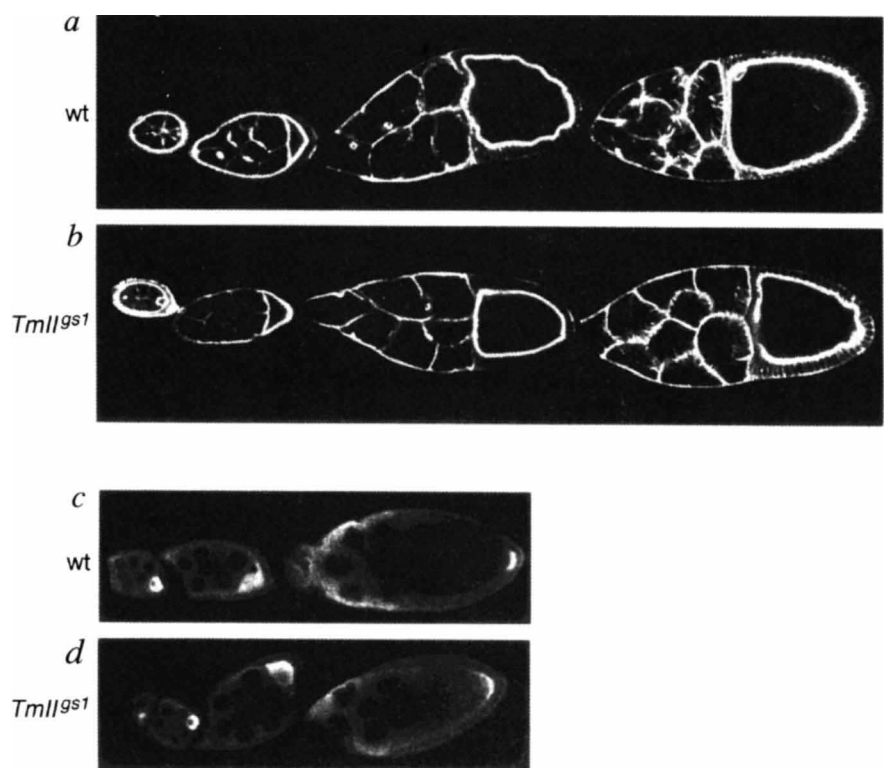


FIG. 2 *osk* RNA and *stau* protein fail to localize to the posterior pole in *TmII^{gs1}* oocytes. In wild-type (a, c, e, g) and *TmII^{gs1}* (b, d, f, h) ovaries, *osk* RNA (a, b) properly accumulates in the developing oocyte, but further localization to the posterior pole is altered in *TmII^{gs1}*. In the mutant, at stage 8 *osk* RNA accumulates at the anterior margin of the oocyte and by stage 10 of development is no longer detected. c, d, Distribution of STAU coincides with that of *osk* RNA. *bcd* (e, f) and *grk* (g, h) RNA distribution seems to be unaffected in *TmII^{gs1}*, as expected, as embryos produced by mutant females show normal head and thorax and dorso-ventral polarity. This indicates that cTm is only required for posterior localization or that its requirement in anterior and dorsal localization is far less important. Oocytes representing relevant stages of oogenesis were chosen from different

ovarioles to produce the composite ovarioles shown in these figures. METHODS. Digoxigenin-labelled DNA probes were used for *in situ* hybridization to ovaries, carried out as described¹. *osk* DNA probe corresponds to the 2.1-kb *SacI* fragment in the *osk* cDNA¹. *bcd* DNA probe corresponds to a 2.5-kb *EcoRI* fragment in *bcd*²⁸. *grk* DNA probe is a *XhoI*-*NotI* fragment from the *grk* cDNA²⁹. Whole-mount antibody stainings of ovaries were detected using biotinylated secondary antibodies and the Elite Kit (Vector Laboratories). After dissection, ovaries were fixed for 10 min in buffered 6% formaldehyde/heptane, permeabilized in methanol:DMSO (9:1), rehydrated into phosphate-buffered saline with 0.1% Triton X-100 (PBT), blocked in PBT/0.5% bovine serum albumin, and incubated with the anti-STAU antibody in blocking solution. Nomarski optics.

FIG. 3 Overall integrity of the cytoskeleton is intact in *Tmll^{gs1}* mutants. Wild-type (a) and *Tmll^{gs1}* (b) ovaries were stained with rhodamine-conjugated phalloidin to visualize filamentous actin. In both wild-type and mutant egg chambers, all three distinct populations of filamentous actin are observed: subcortical actin network in the oocyte, the nurse cells and the follicle cells; ring canals connecting the nurse cells and the oocyte, allowing intercellular transport through the cytoplasmic bridges; and actin filament bundles that assemble in the nurse cells of stage 10b egg chambers and are thought to hold the nurse cell nuclei in position during nurse cell contraction and the subsequent transfer of their cytoplasmic content into the oocyte. Stages from left to right: 6, 8, 10a and 10b. Wild-type (c) and *Tmll^{gs1}* (d) ovaries were stained with an anti-dynein (Dhc64C) antibody. In both wild-type and mutant, dynein protein is enriched in the oocyte and at stage 8 is localized to the posterior pole. a–d, Oocytes representing relevant stages of oogenesis were chosen from different ovarioles to produce the composite ovarioles shown. METHODS. a, b, Ovaries were stained with rhodamine-conjugated phalloidin (Sigma)³⁰; c, d, Ovaries were stained with an anti-dynein (Dhc64C) antibody using a fluorescein-coupled secondary antibody. Images were obtained with the EMBL confocal scanning laser beam microscope (CCM)³¹.



actin, it will be interesting to test whether other actin-binding proteins such as profilin, villin and fascin, encoded by the *Drosophila* genes *chickadee*, *quail* and *singed* (for a review see ref. 21), are also involved in *osk* RNA localization. □

Received 16 May; accepted 25 August 1995.

1. Ephrussi, A., Dickinson, L. K. & Lehmann, R. *Cell* **66**, 37–50 (1991).
2. Kim-Ha, J., Smith, J. L. & Macdonald, P. M. *Cell* **66**, 23–35 (1991).
3. Ephrussi, A. & Lehmann, R. *Nature* **358**, 387–392 (1992).
4. Lehmann, R. & Nüsslein-Volhard, C. *Cell* **47**, 141–152 (1986).
5. Karlik, C. C. & Fyrberg, E. A. *Molec. cell. Biol.* **6**, 1965–1973 (1986).
6. Hanke, P. D., Lepinske, H. M. & Storti, R. V. *J. biol. Chem.* **262**, 17370–17373 (1987).
7. St Johnston, D., Beuchie, D. & Nüsslein-Volhard, C. *Cell* **66**, 51–63 (1991).
8. Pondel, M. D. & King, M. L. *Proc. natn. Acad. Sci. U.S.A.* **65**, 7612–7616 (1988).
9. Pokrywka, N. J. & Stephenson, E. C. *Dev. Biol.* **166**, 210–219 (1994).
10. Sundell, C. L. & Singer, R. H. *Science* **253**, 1275–1277 (1991).
11. Yisraeli, J. K., Sokol, S. & Melton, D. A. *Development* **108**, 289–298 (1990).
12. Theurkauf, W. E., Alberts, B. M., Jan, Y. N. & Jongens, T. A. *Development* **118**, 1169–1180 (1993).
13. Clark, I., Giniger, E., Ruohola-Baker, H., Jan, L. Y. & Jan, Y. N. *Curr. Biol.* **4**, 289–300 (1994).
14. Pokrywka, N. J. & Stephenson, E. C. *Dev. Biol.* **167**, 363–370 (1995).
15. Li, M.-G., McGrail, M., Serr, M. & Hays, T. S. *J. Cell Biol.* **126**, 1475–1494 (1994).
16. Gutzeit, H. *Wilhelm Roux Arch. dev. Biol.* **195**, 173–181 (1986).
17. Squire, J. M. *Trends neuro. Sci.* **66**, 409–413 (1983).
18. Pittenger, M. F., Kazzaz, J. A. & Helfman, D. M. *Curr. Opin. Cell Biol.* **6**, 96–104 (1994).
19. Langford, G. M., *Curr. Opin. Cell Biol.* **7**, 82–88 (1995).
20. Kuznetsov, S. A., Langford, G. M. & Weiss, D. G. *Nature* **356**, 722–725 (1992).
21. Cooley, L. & Theurkauf, W. E. *Science* **266**, 590–595 (1994).
22. Bier, E. et al. *Genes Dev.* **3**, 1273–1287 (1989).
23. Hanke, P. D. & Storti, R. V. *Molec. cell. Biol.* **8**, 3591–3602 (1988).
24. Chou, T.-B., Noll, E. & Perrimon, N. *Development* **119**, 1359–1369 (1993).
25. Wieschaus, E. & Szabad, J. *Dev. Biol.* **68**, 29–46 (1979).
26. Hales, K. H., Meredith, J. E. & Storti, R. V. *Dev. Biol.* **165**, 639–653 (1994).
27. O'Connell, P. O. & Rosbash, M. *Nucleic Acids Res.* **12**, 5495–5511 (1984).
28. Berleth, T. et al. *EMBO J.* **7**, 1749–1756 (1988).
29. Neuman-Silberberg, F. S. & Schupbach, T. *Cell* **75**, 165–174 (1993).
30. Xue, F. & Cooley, L. *Cell* **72**, 681–693 (1993).
31. Stelzer, E. H. K., Stricker, R., Pick, R., Storz, C. & Hänninen, P. *Scanning Imagings* (ed. Wilson, T.) **1028**, 146–151, (proc. Soc. Photo-opt. Instrum. Engng Bellingham, WA, 1989).

ACKNOWLEDGEMENTS. We thank P. Deák for allowing us to test his homozygous viable P insertion lines for grandchildless phenotype, leading to the identification of the *Tmll^{gs1}* allele. We also thank I. Clark and Y. N. Jan for the kinesin-LacZ transgenic fly stocks; T. Schupbach for the *grk* cDNA; T. Hays, R. Lehmann and D. St Johnston for their gifts of dynein, nanos and staufen antisera; and D. St Johnston for their gifts of dynein and staufen antisera; B. Bullard and J. Clayton for the mTm cDNA; R. Harris for help with photography; the EMBL DNA sequencing service for primer synthesis and sequence analysis; N. Gunkel, P. Závorsky and the members of the Ephrussi laboratory for their advice and help during the experiments; and D. Böhm, S. Cohen, M. Giotz, F.-H. Markusen and K. Simons for critical reading of the manuscript. A. G. is a recipient of a predoctoral fellowship from the Ministère de la Recherche et du Travail and M. E. of an EMBO long-term fellowship.

Transient increase in *obese* gene expression after food intake or insulin administration

Régis Saladin*, Piet De Vos*, Michele Guerre-Millo†, Armelle Leturque‡, Jean Girard‡, Bart Staels* & Johan Auwerx*§

* Laboratoire de Biologie des Régulations chez les Eucaryotes, INSERM U325, Institut Pasteur, 1 Rue Calmette, F-59019 Lille, France

† INSERM U177, Institut des Cordeliers, 75006 Paris, France

‡ Ceremod CNRS UPR 1511, 92190 Meudon, France

OBESITY is a disorder of energy balance, indicating a chronic disequilibrium between energy intake and expenditure¹. Recently, the mouse *ob* gene², and subsequently its human and rat homologues^{2,6}, have been cloned. The *ob* gene product, leptin⁷, is expressed exclusively in adipose tissue, and appears to be a signalling factor regulating body-weight homeostasis and energy balance^{2,7–9}. Because the level of *ob* gene expression might indicate the size of the adipose depot, we suggest that it is regulated by factors modulating adipose tissue size. Here we show that *ob* gene exhibits diurnal variation, increasing during the night, after rats start eating. This variation was linked to changes in food intake, as fasting prevented the cyclic variation and decreased *ob* messenger RNA. Furthermore, refeeding fasted rats restored *ob* mRNA within 4 hours to levels of fed animals. A single insulin injection in fasted animals increased *ob* mRNA to levels of fed controls. Experiments to control glucose and insulin independently in animals, and studies in primary adipocytes, showed that insulin regulates *ob* gene expression directly in rats, regardless of its glucose-lowering effects. Whereas the *ob* gene product, leptin, has been shown to reduce food intake and increase energy expenditure^{7–9}, our data demonstrate that *ob* gene expression is increased after